

Test and first validation of FRESCO+

Ping Wang*, Piet Stammes, Nicolas Fournier

Royal Netherlands Meteorological Institute, P.O. Box 201, 3730 AE De Bilt, The Netherlands

ABSTRACT

The FRESCO (Fast Retrieval Scheme for Clouds from the Oxygen A-band) algorithm has been successfully used in GOME and SCIAMACHY cloud retrieval for several years. It simulates the measured reflectance at top of atmosphere at 15 wavelengths at about 758, 761, and 765 nm. The reflectances are pre-calculated, and stored as a look-up-table. The FRESCO products are effective cloud fraction and cloud pressure, which are used in the cloud correction of trace gas retrievals from GOME and SCIAMACHY. Until now only O₂ absorption has been considered in FRESCO. In the new version of the FRESCO algorithm, called FRESCO+, single Rayleigh scattering is added in the reflectance database and the retrieval. Rayleigh scattering is mainly important for the cloud free part of the pixels. The new reflectance database has been tested with DAK (Doubling Adding KNMI) multiple scattering simulations of the O₂ A-band. Applied to GOME data, FRESCO+ gives a global average effective cloud fraction which is about 0.01 larger and a cloud pressure which is about 57 hPa higher than the current FRESCO version. The cloud pressure changes are largest for the less cloudy pixels. The FRESCO+ cloud height has been compared with ground-based cloud observations from the SGP/ARM site.

Keywords: FRESCO+, GOME, SCIAMACHY, cloud fraction, cloud pressure, ARM cloud boundaries

1. INTRODUCTION

FRESCO (Fast Retrieval Scheme for Clouds from the Oxygen A-band) is one of the cloud retrieval algorithms used for GOME and SCIAMACHY [1] (see [2] for a recent overview of GOME cloud detection algorithms). By using oxygen as a well-mixed gas, the cloud pressure can be retrieved in a straightforward way. In FRESCO the cloud pressure and the effective cloud fraction are retrieved from top-of-atmosphere (TOA) reflectances in three 1-nm wide wavelength windows at 758-759, 760-761, and 765-766 nm. The cloud is assumed to be a Lambertian surface with albedo 0.8, and only absorption due to O₂ above the cloud or the ground surface is taken into account. Two light paths are considered in FRESCO: (1) from the sun to the surface and then to the satellite, and (2) from the sun to the cloud top and then to the satellite. The FRESCO cloud algorithm has been validated [3] and the products have been used for cloud correction or cloud masking in retrieval of trace gases, such as O₃ and NO₂. For tropospheric trace gas retrievals the less cloudy pixels (with an effective cloud fraction below about 0.2) are most relevant. Therefore, it is important to optimize FRESCO for the less cloudy pixels. This is done by the addition of single Rayleigh scattering in the retrieval algorithm.

2. PRINCIPLE OF FRESCO+

In FRESCO+ the independent pixel assumption is used. The reflectance (R_{sim}) at TOA is the sum of the reflectances from the cloud-free and cloudy parts of the pixel

$$R_{sim} = cT_cA_c + (1-c)T_sA_s + cR_c + (1-c)R_s \quad (1)$$

where c is the geometric cloud fraction, R_c , R_s , T_c , T_s are the single Rayleigh scattering reflectances and transmittances of cloudy and cloud-free parts of the pixel. T_c , T_s also contain O₂ absorption. R and T are

pre-calculated as a function of solar zenith angle (SZA), viewing zenith angle (VZA), wavelength, and surface or cloud height, and stored as a look-up-table. Cloud top albedo (A_c) is assumed to be 0.8. A_s is surface albedo, taken from climatology.

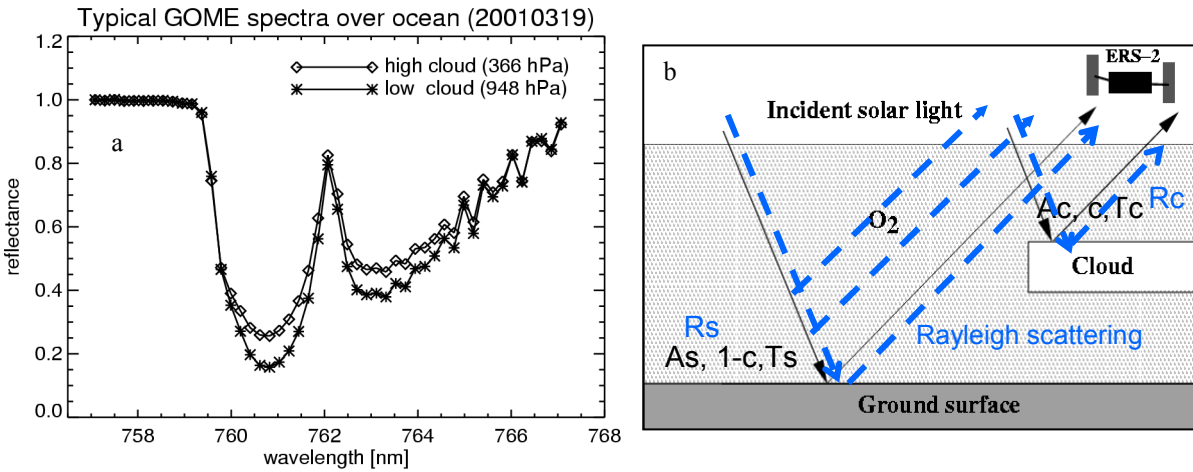


Fig. 1. FRESKO+ principle. (a) O_2 A-band spectra of clouds measured by GOME, (b) FRESKO+ atmospheric model. The cloud and surface are both Lambertian reflectors. Two light paths are considered, from sun to surface to satellite and from sun to cloud to satellite. Single Rayleigh scattering, of which the light paths are dash lines, is taken into account.

3. RESULTS

3.1 Tests of FRESKO and FRESKO+ retrieved cloud heights

We have tested the FRESKO/FRESKO+ cloud retrievals for clear sky scenes and cloudy scenes using simulated reflectances from the DAK model [4,5,6]. In the simulation we assume a surface albedo of 0.1, and no aerosol. The O_2 absorptions are calculated with a line-by-line (LBL) method using HITRAN 2004 [7], which is the same in FRESKO and FRESKO+. The high resolution spectra are convoluted with the SCIAMACHY slit function and interpolated to the SCIAMACHY wavelength grid. The geometries used in this retrieval test are: nadir view, and solar zenith angles 0, 30, 45, 60, 70, and 75 degrees.

For the cloudy scenes, a Henyey-Greenstein phase function with asymmetry factor of 0.85 is used in the simulation. A similarity relation is used in the DAK model to speed up the calculations. The clouds are 1 km thick. The other settings are the same as for the cloud free scenes. Three types of cloudy scenes are simulated: a) single layer clouds, b) single layer clouds at two different heights and c) two-layer clouds. The FRESKO(+) retrieved cloud heights at SZA = 45 degree are listed in Table 1.

The resulting cloud fractions retrieved by FRESKO from the clear sky DAK spectra are as expected, almost 0. However, the FRESKO retrieved cloud heights are close to 8 km. The reason for these large cloud heights is that the Rayleigh scattering by air molecules is included in the DAK model, but not in FRESKO. So the reflectances inside the O_2 A-band (at 761 and 765 nm) are larger than that of a purely absorbing O_2 atmosphere. Using the same clear sky DAK spectra as input, the cloud fractions retrieved by FRESKO+ are again 0 (less than 0.01) but the cloud heights are about 0.5 km, which is much more reasonable than the FRESKO results. The remaining 0.5 km error in cloud height for the cloud free scenes is due to the contribution of multiple scattering in the simulated spectra. So we may expect that FRESKO+ will give better cloud height results for less cloudy scenes than FRESKO.

Fig. 2 shows the results of the FRESKO(+) retrieved cloud heights for the three kinds of cloudy scenes as a function of solar zenith angle. The FRESKO(+) retrieved cloud height is somewhere inside the cloud for single layer clouds (Fig. 2a). For single-layer clouds at two altitudes and for two-layer clouds, FRESKO(+) cloud height is between the two layers (Fig. 2b,c). In the O₂ A-band photons can penetrate to some distance into the clouds. Therefore the retrieved cloud height depends on the cloud optical and geometrical thickness. FRESKO+ cloud heights are lower than the FRESKO cloud height due to the single Rayleigh scattering. The FRESKO(+) cloud height is higher at large SZA. At large SZA the light path are more slant than at the small SZA, so the light penetrate less deep in the vertical direction of clouds.

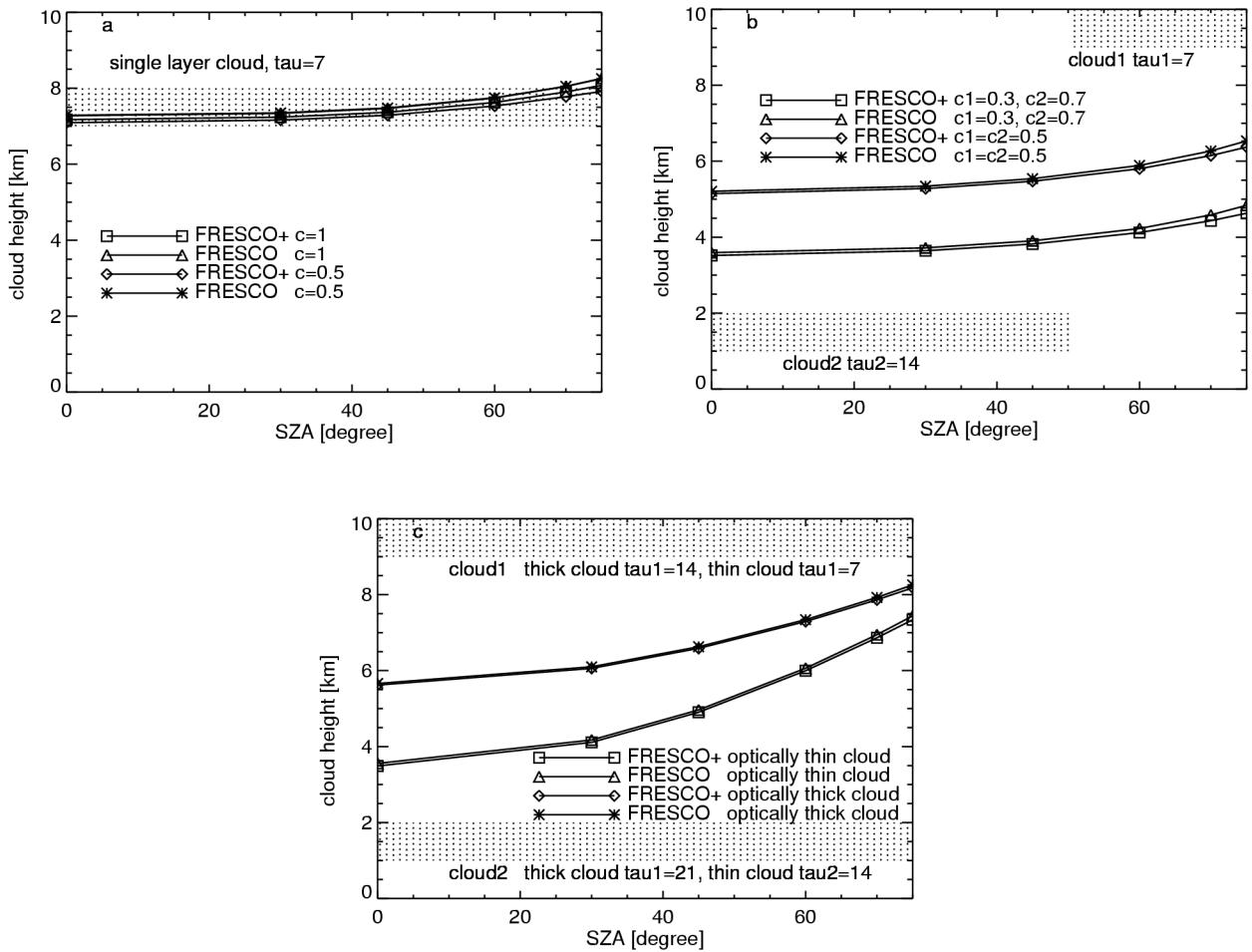


Fig. 2. FRESKO(+) retrieved cloud heights using simulated spectra from a LBL multiple scattering model. Henyey-Greenstein phase function with g of 0.85 is assumed. Cases: (a) single-layer clouds, (b) single-layer clouds at two heights, (c) two-layer clouds.

Table 1. FRESCO(+) retrieved cloud height for cloudy scenes simulated by DAK. Here SZA=45 degree, nadir view. Tau, C, H are cloud optical thickness, geometric cloud fraction and cloud height (bottom – top). The number ‘1’ is for higher cloud, ‘2’ is for lower cloud when there are two cloud heights.

case	Cloud free	Single-layer clouds		Single-layer clouds at two heights		Two-layer clouds	
Cloud settings	Clear scene C=0 H=0	Tau=7 C=1 H=7-8km	Tau=7 C=0.5 H=7-8km	Tau1=7 C1=0.3 H1=9-10km Tau2=14 C2=0.7 H2=1-2km	Tau1=7 C1=0.5 H1=9-10km Tau2=14 C2=0.5 H2=1-2km	Tau1=7 C1=1 H1=9-10km Tau2=14 C2=1 H2=1-2km	Tau1=14 C1=1 H1=9-10km Tau2=21 C2=1 H2=1-2km
FRESCO+ Cloud height (km)	0.528	7.367	7.288	3.820	5.472	4.904	6.586
FRESCO Cloud height (km)	7.906	7.492	7.480	3.905	5.541	4.965	6.628

3.2 FRESCO+ results for GOME measurements

The FRESCO+ algorithm has been applied to GOME data and compared to FRESCO results. The GOME data used in this paper are reprocessed GOME level 1 data using the extraction program GDP 2.4 from DLR. In this paper we use GOME measurements of 16 July 1997 as an example. In FRESCO and FRESCO+ the surface albedo database is 0.25x0.25 degrees with the albedo correction for deserts [8]. The surface height database is also 0.25x0.25 degrees resolution. HITRAN 2004 is used in the calculation of transmission databases. The only difference between FRESCO and FRESCO+ is single Rayleigh scattering.

The histograms of effective cloud fraction and cloud pressure from FRESCO+ and FRESCO are shown in Fig. 3. The averaged effective cloud fraction is 0.341 in FRESCO+ and 0.326 in FRESCO on 16 July 1997. There are more pixels having small effective cloud fractions, so mostly the geometric cloud fractions are small or the clouds are optically thin. The peak at effective cloud fraction 1 occurs because of the cloud albedo larger than 0.8. The peak in cloud pressure at 120-140 hPa bin is because in FRESCO the lowest cloud pressure is 130 hPa; all the cloud pressures lower than 130 hPa are set to 130 hPa. There are more low clouds than high clouds globally. For FRESCO+, most of the clouds are at 850 hPa, however in FRESCO most clouds are at 800 hPa.

The statistics of the effective cloud fraction and cloud pressure differences between FRESCO+ and FRESCO on 16 July 1997 are shown in Fig. 4. The mean difference in effective cloud fraction is 0.013 (sigma= 0.020) and the mean difference in cloud pressure is 57 hPa (sigma=85 hPa). On other days the differences are similar: e.g. on 1 September 1997 and 1 March 2000 the effective cloud fraction differences are 0.01 and 0.012, respectively, and the cloud pressure differences are 56 and 51 hPa, respectively. Therefore, we estimate that the effective cloud fraction is about 0.01 larger in FRESCO+ and the cloud pressure is about 57 hPa higher than in FRESCO. Since the effect of single Rayleigh scattering is more important for the less cloudy pixels, we expect that the change in cloud pressure is different for less cloudy and fully cloudy pixels. This can be seen from Fig. 5, which shows the globally averaged

retrieved cloud pressure as a function of effective cloud fraction for FRESKO+ and FRESKO. For the small effective cloud fractions, say less than 0.1, the cloud pressure differences between FRESKO+ and FRESKO are 100-200 hPa. When the effective cloud fraction gets larger, the cloud pressure differences becomes smaller, less than 50 hPa.

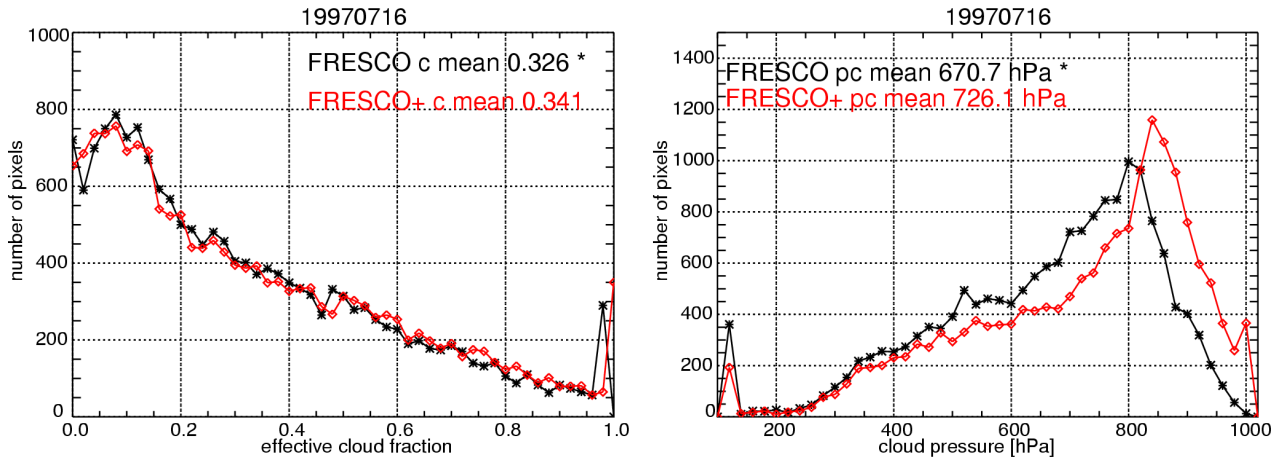


Fig. 3. Histogram of effective cloud fraction (left) and cloud pressure (right) from FRESKO (line with asterisk mark) and FRESKO+ (line with diamond mark) for GOME data of 16 July 1997.

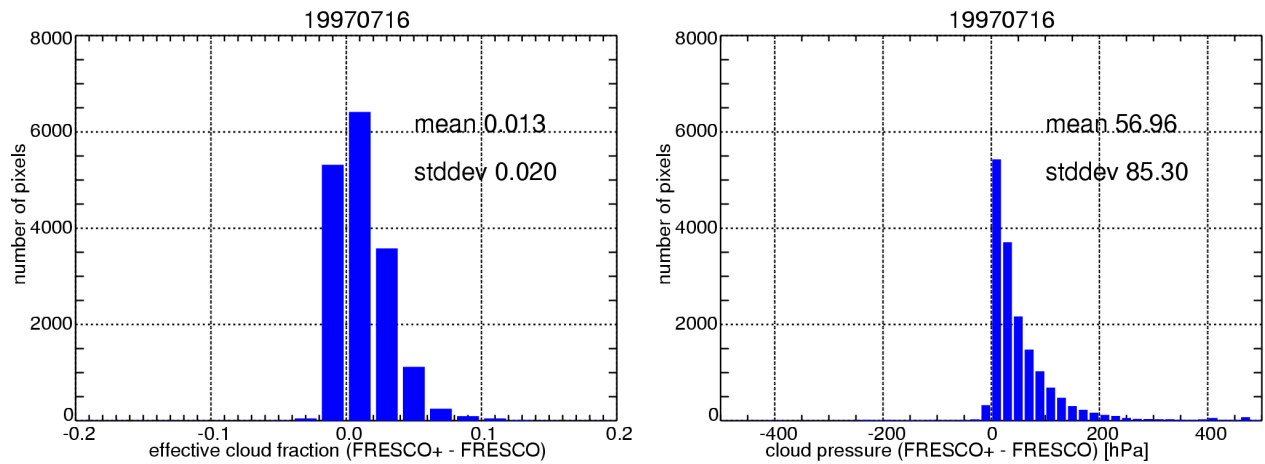


Fig. 4. Histogram of the effective cloud fraction differences (left) and cloud pressure differences (right) FRESKO+ - FRESKO, for GOME data of 16 July 1997.

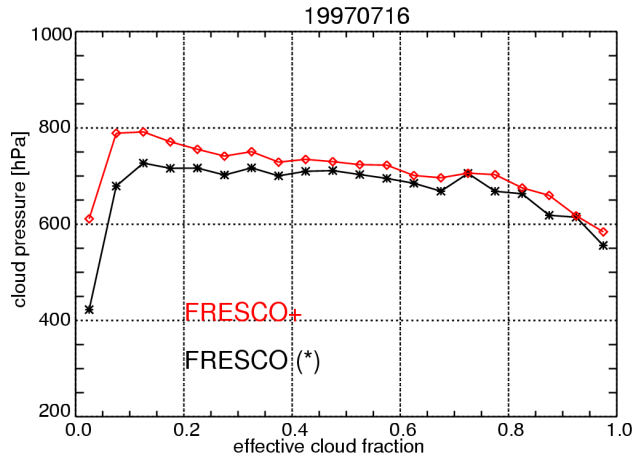


Fig. 5. The globally averaged cloud pressure as a function of effective cloud fraction, in 0.05 effective cloud fraction bins, for GOME measurements on July 16, 1997. The curve with diamond is the FRESKO+ result, the curve with asterisk mark is the FRESKO result.

3.3 Comparison with ARM site cloud height data

FRESKO+ cloud height has been compared with ARM (Atmospheric Radiation Measurement) active remote sensing cloud boundaries data at SGP (Southern Great Plains) [9]. The GOME pixel size is 40 km x 320 km which is not easy to compare with Lidar/Radar data. The FRESKO+ GOME cloud height in 1997 and 2000 are compared to the cloud height measured at SGP. The SGP/ARM data within two hours of the GOME overpass time (10:30 local time) and with cloud cover longer than one hour are selected. We calculate the histogram of SGP cloud height in the collocated GOME pixel. For the single layer clouds we compare with the middle of the cloud; for multiple-layer clouds we compare with the average of the cloud top for the two main layers. The preliminary result is shown in Fig. 6. Over the SGP/ARM site there are not many single layer clouds. Most of the FRESKO cloud heights are lower than the Lidar/Radar cloud top height, which agrees with the DAK simulated results shown in section 3.1. However with our selection criterion it is possible that the Lidar/Radar cloud heights are not representative for the clouds in the GOME pixel.

4. CONCLUSIONS

In this paper we explained the principle of FRESKO+. The reflectance spectra with single Rayleigh scattering are compared to DAK model simulations for clear sky scenes, which show better agreement than a purely absorbing atmosphere as is used in FRESKO. The FRESKO+ algorithm is tested with simulated spectra and GOME spectra. Due to the addition of single Rayleigh scattering in FRESKO+, the change in effective cloud fraction is very small, about 0.01. However, the cloud pressure is improved largely for less cloudy pixel. On average the cloud pressure is about 57 hPa higher in FRESKO+ than in FRESKO. The difference in cloud pressure is larger for the less cloudy pixels than for the fully cloudy pixels. So, including single Rayleigh scattering improved FRESKO for less cloudy pixels, which are most relevant for the observation of tropospheric pollution.

The comparison of FRESKO+ cloud height with SGP/ARM cloud height shows a reasonable correlation, $r=0.8$. However there are still some differences, especially for multi-layer clouds. As a preliminary result, it is promising. The results could be better if we could consider the ARM cloud optical thickness and using satellite O₂ A-band data with better spatial resolution such as SCIAMACHY and GOME-2.

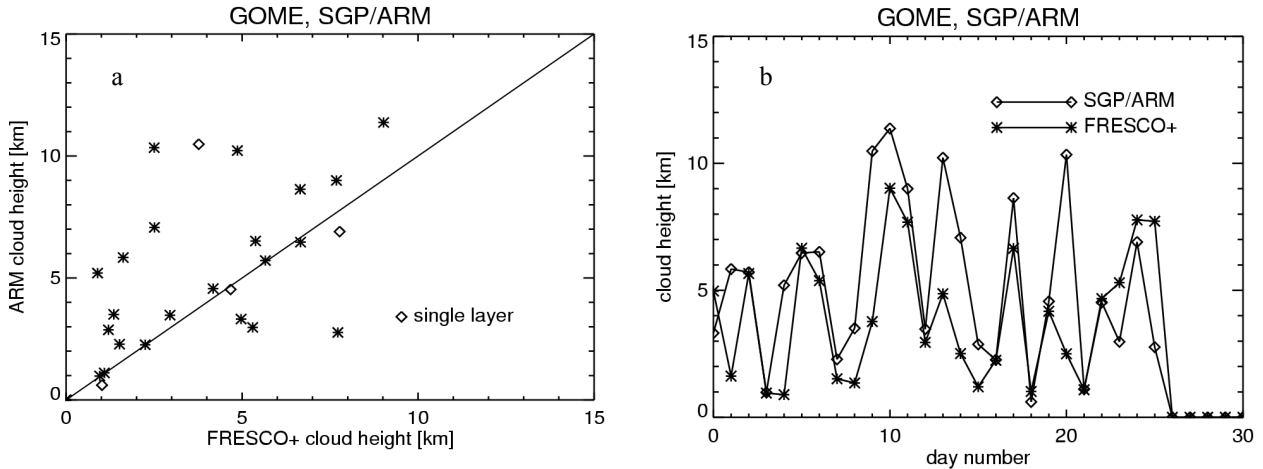


Fig. 6. Comparison between FRESCO+ cloud height and SGP/ARM site cloud height. (a) FRESCO+ and ARM cloud height. (b) FRESCO+ and SGP/ARM cloud height time series. The measurements in the entire year 1997 and 2002 were used for the GOME and SGP collocation.

ACKNOWLEDGEMENTS

GOME GDP 2.4 software was provided by DLR (German Aerospace Center). ARM data is made available through the U.S. Department of Energy as part of the Atmospheric Radiation Measurement Program. Funding was provided by the Netherlands Institute for Space Research (SRON) through the FRESCO+ project (EO-067).

REFERENCES

1. R. B. A. Koelemeijer, P. Stammes, J. W. Hovenier, and J. F. de Haan, 2001, A fast method for retrieval of cloud parameters using oxygen A-band measurements from the Global Ozone Monitoring Experiment, *J. Geophys. Res.*, *106*, 3475–3490.
2. M. Grzegorski, M. Wenig, U. Platt, P. Stammes, N. Fournier, T. Wagner, 2006, The Heidelberg iterative cloud retrieval utilities (HICRU) and its application to GOME data, *ACPD* 1679-1723, SRef-ID: 1680-7375/acpd/2006-6-1679.
3. R. B. A. Koelemeijer, P. Stammes, J. W. Hovenier, and J. F. de Haan, 2002, Global distributions of effective cloud fraction and cloud top pressure derived from oxygen A-band spectra measured by the Global Ozone Monitoring Instrument: Comparison to ISCCP data, *J. Geophys. Res.*, *107* (D12), doi 10.1029/2001JD000840.
4. N. Fournier, P. Stammes, and M. Eisinger, Development of a polarised radiative transfer model in the oxygen A-band for satellite retrieval of cloud top pressure, *Proceedings of IRS 2004: Current Problems in Atmospheric Radiation*, Eds. H. Fischer and B.-J. Sohn, A. Deepak Publishing, Hampton (VA), 2006, pp. 183.
5. J. De Haan, F. P. B. Bosma, and J. W. Hovenier, The adding method for multiple scattering calculations of polarized light, *Astron. Astrophys.*, *183*, 371-391, 1987.
6. P. Stammes, Spectral radiance modelling in the UV-visible range, in *IRS 2000: Current Problems in Atmospheric Radiation*, edited by W. Smith and Y. Timofeyev, pp. 385-388, A. Deepak, Hampton, Va, 2001.
7. L. S. Rothman, Jacquemart, D., Barbe, A., et al.: The HITRAN 2004 molecular spectroscopic database, *Journal of Quantitative Spectroscopy & Radiative Transfer* *96*, 139–204, 2005.

8. N. Fournier, P. Stammes, M. de Graaf, R. van der A, A. Piders, M. Grzegorski, A. Kokhanovsky, Improving cloud information over deserts from SCIAMACHY Oxygen A-band measurements, ACP, p163-172, 2006, SRef-ID: 1680-7324/acp/2006-6-163.
9. E. E. Clothiaux, T. P. Ackerman, G. G. Mace, K. P. Moran, R. T. Marchand, M. A. Miller, and B. E. Martner, Objective determination of cloud heights and radar reflectivities using a combination of active remote sensors at the ARM CART sites, J. Appl. Meteorol., 39, 645– 665, 2000.